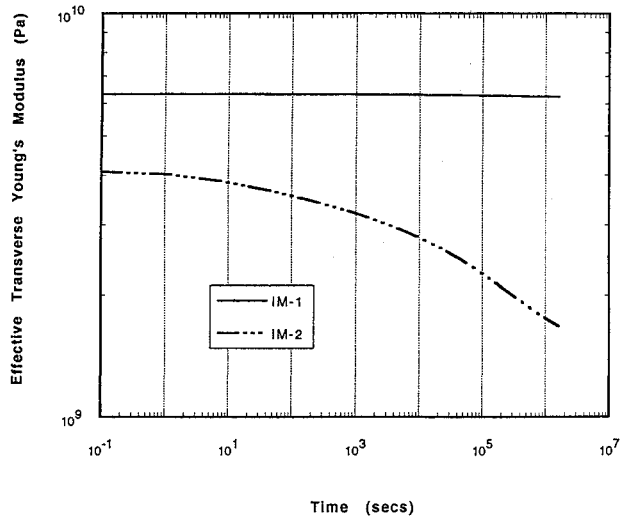

Fig. 3 Effective transverse Young's modulus of composite with elastic matrix.

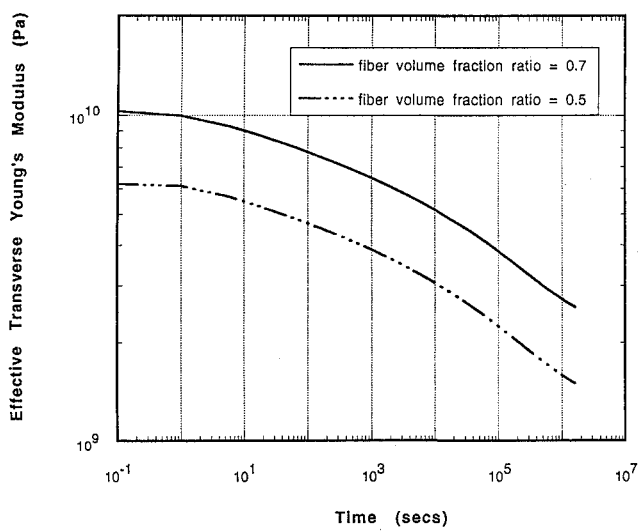

Fig. 4 Effective transverse Young's modulus of composite with viscoelastic matrix.

modulus drops by only 2% with an 80% decrease in the interfacial modulus. However, with material IM-2 representing the interphase, the value of the transverse effective Young's modulus decreases by 58.8% during 1.6×10^6 s time period. The effective transverse Young's modulus is plotted in Fig. 3. In this case, the strains in the fiber decrease with time whereas those in the matrix increase. As time grows, the modulus of the interphase degrades to a much smaller value than that of the fiber or matrix. The interface becomes very weak, and this could be interpreted as approaching a state of debonding.

In a second study, the constitutive relations for the interfacial layer and the matrix are viscoelastic, and the fiber is elastic. The volume ratio of the fiber is 0.7, and the interphase thickness is $0.05l$. The number of elements and degrees of freedom are the same as those in the first study. IM-1 is used for the interfacial material. Time-dependent responses in the fiber, interphase, and matrix are calculated. Transverse strain in the matrix increases 56% during a 1.5×10^6 s period whereas the Young's modulus of the matrix decreases by 78%. Another study comprises a fiber-reinforced composite with volume fraction $v_f = 0.5$. Fiber, interphase, and matrix properties are given in the second example. Effective Young's moduli in the transverse direction are computed and are depicted in Fig. 4. The effective transverse Young's modulus is significantly affected by the fiber volume fraction and viscoelastic behavior of the matrix.

References

[1]Papanicolaou, G. C., Paipetis, S. A., and Theocaris, P. S., "The Concept of the Boundary Interphase in Composite Mechanics," *Colloid and Polymer Science,* Vol. 256, July 1978, pp. 333–348.

[2]Hashin, Z., "Thermoelastic Properties of Fiber Composites with Imperfect Interface," *Mechanics of Materials,* Vol. 8, 1990, pp. 333–348.

[3]Gosz, M., Moran, B., and Achenbach, J. D., "Effect of a Viscoelastic Interface on the Transverse Behavior of Fiber-reinforced Composites," *International Journal of Solids and Structures,* Vol. 27, No. 14, 1991, pp. 1757–1771.

[4]Lin, K. Y., and Yi, S., "Analysis of Interlaminar Stresses in Viscoelastic Composites," *International Journal of Solids and Structures,* Vol. 27, No. 7, 1991, pp. 929–945.

[5]Yi, S., "Thermoviscoelastic Analysis of Delamination Onset and Free Edge Response in Epoxy Matrix Composite Laminates," *AIAA Journal,* Vol. 31, No. 12, 1993, pp. 2302–2328.

[6]Lekhnitskii, S. G., *Theory of Elasticity of an Anisotropic Body,* Holden-Day, San Francisco, CA, 1963.

Submodeling Approach to Adaptive Mesh Refinement

John O. Dow*
University of Colorado, Boulder, Colorado 80309
and
Matthew J. Sandor†
Storage Technology Corporation, Louisville, Colorado 80028

Introduction

ERRORS exist in finite element results in regions where the underlying piecewise polynomials cannot replicate the exact solution. Zienkiewicz and Zhu[1] have shown that these discretization errors can be estimated by comparing the discontinuous finite element stress fields to smoothed stress fields developed from the finite element results. The errors in individual elements are quantified as the strain energy contained in the differences between the two stress fields.

The finite element solution is improved by refining the mesh in regions of high error and solving the problem again. This adaptive refinement process is repeated until an acceptable level of accuracy is achieved. In the Zienkiewicz and Zhu approach, this iterative process is terminated when the global error, which is computed as the sum of the elemental errors, reaches a prespecified level.

This paper presents two improvements to the adaptive refinement scheme just described: 1) instead of reanalyzing the whole region, only regions of interest such as stress concentrations are reanalyzed and 2) instead of terminating the adaptive refinement using a criterion based on the global error, a local error criterion is used. The first modification has the advantage of focusing the computational efforts where they belong. The second modification has the advantage of insuring that the solution is accurate in critical regions.

The first improvement is accomplished by identifying an internal boundary that passes through elements with a low level of error. The subproblem defined by this process is refined, the displacements from the previous analysis are imposed on the internal boundary, and the new model is solved. The second improvement terminates the local adaptive refinement process when the elemental errors in the subproblem reach a prespecified level. These changes improve the efficiency of the analysis and ensure that the accuracy of the results in the critical region is acceptable. All of the computations, including the automated mesh refinements, are performed within a commercial finite element code.

Received July 24, 1993; revision received June 20, 1994; accepted for publication June 24, 1994.

*Associate Professor, Department of Civil, Environmental and Architectural Engineering. Member AIAA.

†Senior Development Engineer. Senior Member AIAA.

Theoretical Background and Internal Boundary Definition

The energy error norm for an element is defined as

$$|e_i|^2 = \int_\Omega \{\sigma^* - \sigma'\}^T D^{-1} \{\sigma^* - \sigma'\} \, d\Omega \tag{1}$$

where σ' is the stress vector found by the finite element model, σ^* is the smoothed stress vector, and Ω is the area of the ith element. The smoothed stresses are formed by interpolating the averaged stresses at the nodes over the individual elements using the finite element displacement interpolation functions.[2,3]

The percentage of error in an individual element is defined as

$$E_i = \left[\frac{e_i}{U_i + e_i}\right]^{\frac{1}{2}} * 100 \tag{2}$$

where U_i is the strain energy in the ith element and e_i is the energy error norm in the ith element. The global percentage of error is defined similarly. Each of the quantities in Eq. (2) is a summation over all of the elements.

The critical issues in this submodeling process are the following: 1) to identify internal submodel boundaries such that accurate solutions are produced and the efficiency is enhanced and 2) to identify termination criteria that guarantee a well-converged solution.

In this work, an elemental error of 5% or less is arbitrarily chosen to define an element with an acceptable error. This 5% criterion is used both to define the location of the internal boundary and to stop the adaptive refinement process. As will be seen in the results that follow, this arbitrary, nonoptimum criterion demonstrates the proof of concept of the idea of adaptively refining a subproblem.

The internal boundary is defined in the following way. The initial finite element model is solved, and an error analysis is performed. A circle is defined that has its origin at a point of critical interest in the analysis and a radius that encompasses all of the elements with 5% error in the region of interest. This process is shown in Fig. 1a for the case of a one-quarter symmetry model of a shear panel with a circular hole. The numbers superimposed on the elements indicates the percentage of error in the element. As can be seen, the internal boundary isolates a region with a maximum error of 5%.

The boundary of the submodel consists of a combination of an internal boundary and a portion of the external boundary of the original problem. Displacements interpolated from the global model are applied to the internal boundary to include the effects of the remainder of the problem. This initial internal boundary can be retained throughout the remainder of the analysis, or the radius can be reduced further as the elements on the edge of the circle contain less error. The use of a moving internal boundary reduces the total area that is contained in the submodel and adds to the efficiency of the analysis. The process is terminated when the maximum elemental error is 5%. The evolution of this approach is discussed in detail in Ref. 4. Other approaches for defining an internal boundary are, of course, possible.

The test problem consists of a square shear panel with an interior hole. In the first problems solved, the hole is circular. In later examples, ellipses with more severe stress concentrations are evaluated. An initial mesh representing one-quarter of the circular hole problem of unit thickness is shown in Fig. 1a. The analytic solution of this problem with an elliptic hole in a finite shear panel is given in Ref. 5. Six-node linear strain elements are used to represent these plane stress problems because refined meshes are easy to develop, curved boundaries can be included in the model, and no artificial stiffening due to parasitic shear is present.[6]

Isotropic linear elastic properties are used. The two independent material constants are assumed to be $E = 30.0 \times 10^6$ psi and $\nu = 0.3$. The geometry and the loading condition allow a one-quarter symmetric representation to be used. On the edge where the load is applied, the displacement in the x direction is uniform with a loading of 5000 lb applied to the master node. This is similar to a uniform load of 1000 lb/in. along the edge.

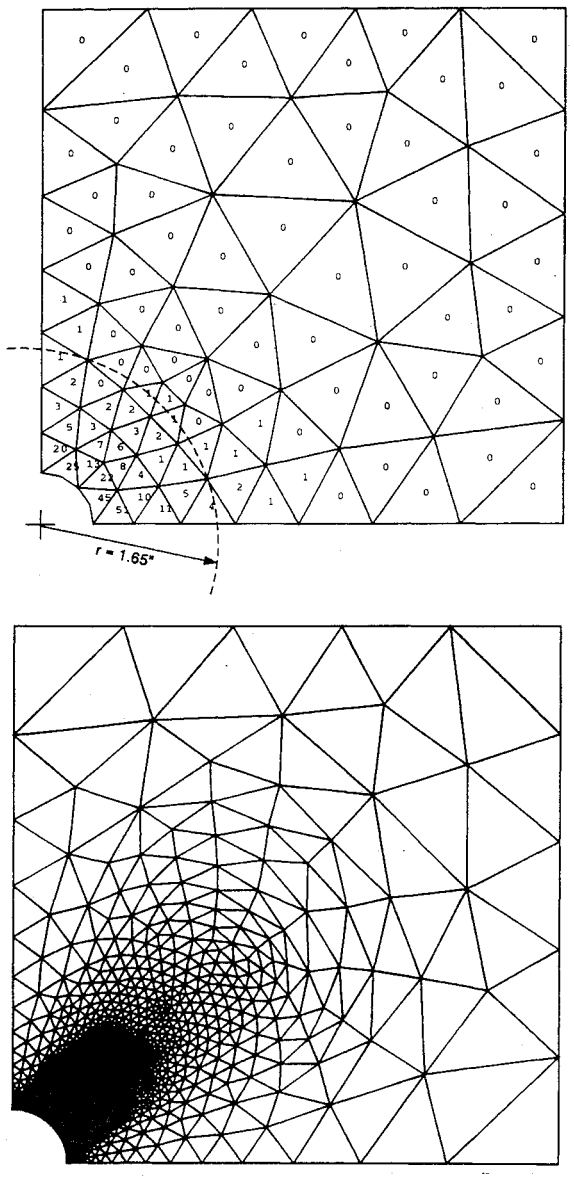

Fig. 1 Initial mesh with fixed internal boundary 430 DOF and the final global refinement for a circular hole problem 11,454 DOF.

Full Model Refinement

The original quarter symmetry model for the circular hole containing 430 degrees of freedom (DOF) is shown in Fig. 1a with the percent elemental error norms. The maximum stress of 2688 psi is 11.7% less than the theoretical maximum stress of 3047 psi. The global error norm for the model is 3.9%. If the quality of the result were to be judged in terms of the global error norm and in the absence of a known solution, it might be concluded that the stress results produced by this analysis are acceptable. However, the elemental error norms presented in Fig. 1a indicate that large errors exist in the elements adjacent to the hole. The maximum elemental error is 51.1%. The maximum error is not located in the region of the maximum stress. Close analysis of the stresses show that large errors exist in the shear stresses.

This model is globally refined until the maximum elemental error is 5%. The peak value of σ_x is 3020 psi which is 0.9% less than the analytic solution. The final finite element model contains 11,454 degrees of freedom and is shown in Fig. 1b. The aggregate results of these refinements are given in Table 1.

It is interesting to note that the peak stress found in the first refinement agrees with theory to within 2.1%. This means that the subsequent refinements are probably not needed. It should be noted that the analytic solution is not available for most problems and so the accuracy of the approximate solution must be confirmed in other ways. This can be accomplished by evaluating the change

Table 1 Results for a globally refined model

DOF	Max. elem. error, %	$(\sigma_x)_{max}$, psi	Stress error, %	Global error, %
430	51.1	2,690	11.72	3.9
1,362	21.6	2,985	2.03	0.6
2,150	13.2	3,000	1.54	0.4
5,606	7.2	3,015	1.05	0.3
9,958	5.1	3,020	0.89	0.2
11,454	4.0	3,020	0.89	0.2

Table 2 Results for a locally refined model

DOF	Max. elem. error, %	$(\sigma_x)_{max}$, psi	Stress error, %
282	25.0	2,984	2.07
442	20.0	2,977	2.29
942	12.9	3,005	1.38
4,466	7.2	3,017	0.98
9,174	5.1	3,018	0.95
11,394	4.0	3,018	0.95

in the peak stress from refinement to refinement or by specifying an elemental error criterion. In either case, the third and, perhaps, the fourth iterations would have to be performed before convergence could be assumed. The third iteration has five times as many DOF as the original mesh, and the fourth has 13 times as many. As can be seen in the final column of Table 1, the global errors are not closely correlated to the errors in the maximum stresses. For this reason, the global error is not indicative of the accuracy of the critical quantities and will not be presented for the remainder of the analyses.

An evaluation of the elemental error distribution in the original mesh shows that 350 of the original 430 DOF (81.4%) are associated with the low error elements (5% or less elemental error). Since solution times are related to the square of the problem size, it can be seen that a penalty is paid for retaining unnecessary portions of the problem.

Fixed Internal Boundary

As was just seen, the reanalysis of the total problem contained a large region that did not need to be reanalyzed. The errors in this region were low. The available computational resources could be better expended on the critical part of the problem where the stresses and errors are higher if the region of low error is removed from the subsequent analyses.

A large portion of the region of low error is separated from the original problem with an interior boundary that consists of the arc of radius of 1.65 in. shown in Fig. 1a. The origin of the arc coincides with the center of the interior hole and the radius encompasses the element farthest from the center with an error measure of 5%. This provides an internal boundary that accurately represents the effect of the remainder of the problem on the submodel. The results of successively refining this submodel are given in Table 2. As can be seen, the critical stress for even the initial refinement correlates well with the exact result. The accuracy of the results shown in Table 2 indicate that the interpolation of the displacements on the internal boundary from the initial solution of the whole problem accurately imposes the effects of the remainder of the problem on the subproblem.

The distribution of the elemental errors in the first four refinements of the subproblem are shown in Fig. 2. As the refinement progresses, more and more of the region is populated by elements with little or no error. This suggests that the internal boundary need not be fixed and that the computational efficiency could be enhanced by introducing a strategy with a moving internal boundary.

Floating Internal Boundary

Two different floating boundary schemes were evaluated. Originally, the origin of the circular boundary coincided with the center of the hole. However, preliminary studies showed that a wider range of problems could be satisfactorily analyzed by the moving boundary strategy if the center of the arc was located at the point of maximum stress.[4] In strategies involving moving boundaries, the boundary conditions are interpolated from the previous, locally refined mesh instead of from the original global model. This approach was shown to be necessary if accurate results were to be achieved.[4] The results of this strategy for the circular hole are shown in Table 3.

Table 3 Results for a locally refined model with a moving internal boundary

DOF	Max. elem. error, %	$(\sigma_x)_{max}$, psi	Stress error, %
1,400	26.6	2,926	3.97
1,356	19.5	2,975	2.36
1,282	15.2	2,989	1.90
1,218	13.1	2,989	1.90
2,946	9.1	3,002	1.48
5,402	5.3	3,009	1.25
5,160	4.6	3,009	1.25

Table 4 Results for a globally refined 2:1 model

DOF	Max. elem. error, %	$(\sigma_x)_{max}$, psi	Stress error, %
672	59.7	2,956	41.1
1,430	59.7	3,246	35.3
2,104	56.4	3,743	25.4
3,740	18.4	4,730	5.7
5,060	11.8	4,900	2.3
5,432	9.2	4,952	1.3

When these results are compared to the previous two solutions of this problem, two observations concerning accuracy can be made. First, it is seen that approximately the same number of DOF are required to achieve the same level of accuracy in the maximum stress. Stress errors of 1.25% or less are found by the three approaches with models consisting of 5606, 4466, and 5160 DOF, respectively. Second, it is seen that substantially fewer DOF are required to achieve the specified level of 5% for the maximum elemental error with the floating boundary approach than for the other two approaches. Only 5160 DOF are required: 11,454 and 11,394 for the global model and the fixed internal boundary model, respectively.

In the case of a 2:1 elliptical stress concentration, the floating boundary approach requires substantially fewer DOF to achieve both a given level of error in the maximum stress and the 5% maximum elemental error criterion.[4] Thus, it can be concluded that the approach of adaptively refining a local model with a moving boundary centered at the point of maximum stress produces efficient and accurate results.

Applications

The approach using a floating interior boundary centered at the point of maximum stress will now be applied to other problems. The procedure will be applied to stress concentrations in elliptical holes with aspect ratios of 2:1, 5:1, and 10:1, respectively.

The initial global model of the 2:1 stress concentration contains 672 DOF and yields a peak x component of stress of 2956 psi. The analytic result is 5017 psi so the stress error is 41%. The model has a maximum elemental error of 60%.

When the global model is refined with the 5% elemental error as the target, the results are as shown in Table 4. As can be seen, sufficiently accurate results were obtained before the elemental error criterion was reached. With a final refinement of 5432 DOF, a peak stress of 4952 psi is predicted. This is 1.3% less than the analytic solution.

When the floating radius internal boundary approach is applied to the 2:1 problem, the results are as shown in Table 5. After seven refinements, the peak x-component stress is 4954 psi which is 1.26% less than the exact solution. This result was achieved with a model containing 2802 DOF. This is approximately one-half of the size of the model needed to achieve a comparable accuracy by refining the global model.

The coarse global model of the 5:1 stress concentration contains 246 DOF and a peak x-component stress of 3224 psi. The analytic result is 10,948 psi so the finite element stress value is more than three times smaller than the actual value. This corresponds to a stress error of 70.6%, a maximum elemental error of 74% and a global error of 11.3%. As is typical, the maximum error is near the hole and the errors drop off rapidly away from the hole.

The results of refining the problem with the floating interior boundary centered at the point of maximum stress are summarized in Table 6. After seven refinements, a peak x component of stress of 10,507 psi is predicted. This is 4.03% less than the theoretical value. This result was achieved with a mesh of 6,736 DOF and a maximum elemental error of 3.6%.

This configuration was not globally refined so there is no basis for directly establishing the efficiency of the moving boundary technique for this problem. However, based on the average element size in the final refinement, the problem size for a uniformly refined mesh can be estimated as follows. Inspection of the final mesh refinement for the 5:1 ellipse implies that a uniformly refined mesh would contain approximately 1.125×10^7 DOF. If an adjustment of, say, 100 is made to allow for a transition to larger elements toward the boundary (for the 1:1 geometry, an adjustment factor of 67 was found), the full model would contain approximately 112,500 DOF. Thus, it is concluded that for the 5:1 stress concentration, the submodeling based adaptive refinement procedure provides for a substantial reduction in the number of DOF required to accurately represent this problem.

The results of applying the procedure to the stress concentration consisting of a 10:1 ellipse produces the results shown in Table 7. After eight refinements, a peak stress component in the x direction

Table 5 Results for a locally refined 2:1 model with a moving internal boundary

DOF	Max. elem. error, %	$(\sigma_x)_{max}$, psi	Stress error, %
246	74.0	3,224	70.55
592	65.7	3,797	24.32
754	27.2	4,511	10.09
720	18.7	4,774	4.84
644	11.8	4,853	3.27
666	10.0	4,889	2.55
1,326	7.3	4,938	1.58
2,802	3.8	4,954	1.26

Table 6 Results for a locally refined 5:1 model with a moving internal boundary

DOF	Max. elem. error, %	$(\sigma_x)_{max}$, psi	Stress error, %
246	74.0	3,224	70.55
1,264	80.9	5,651	48.38
1,630	34.7	8,102	26.00
1,718	19.4	9,405	14.09
1,586	15.1	9,838	10.14
1,468	13.0	9,988	8.77
3,172	8.2	10,294	5.97
6,736	3.6	10,507	4.03

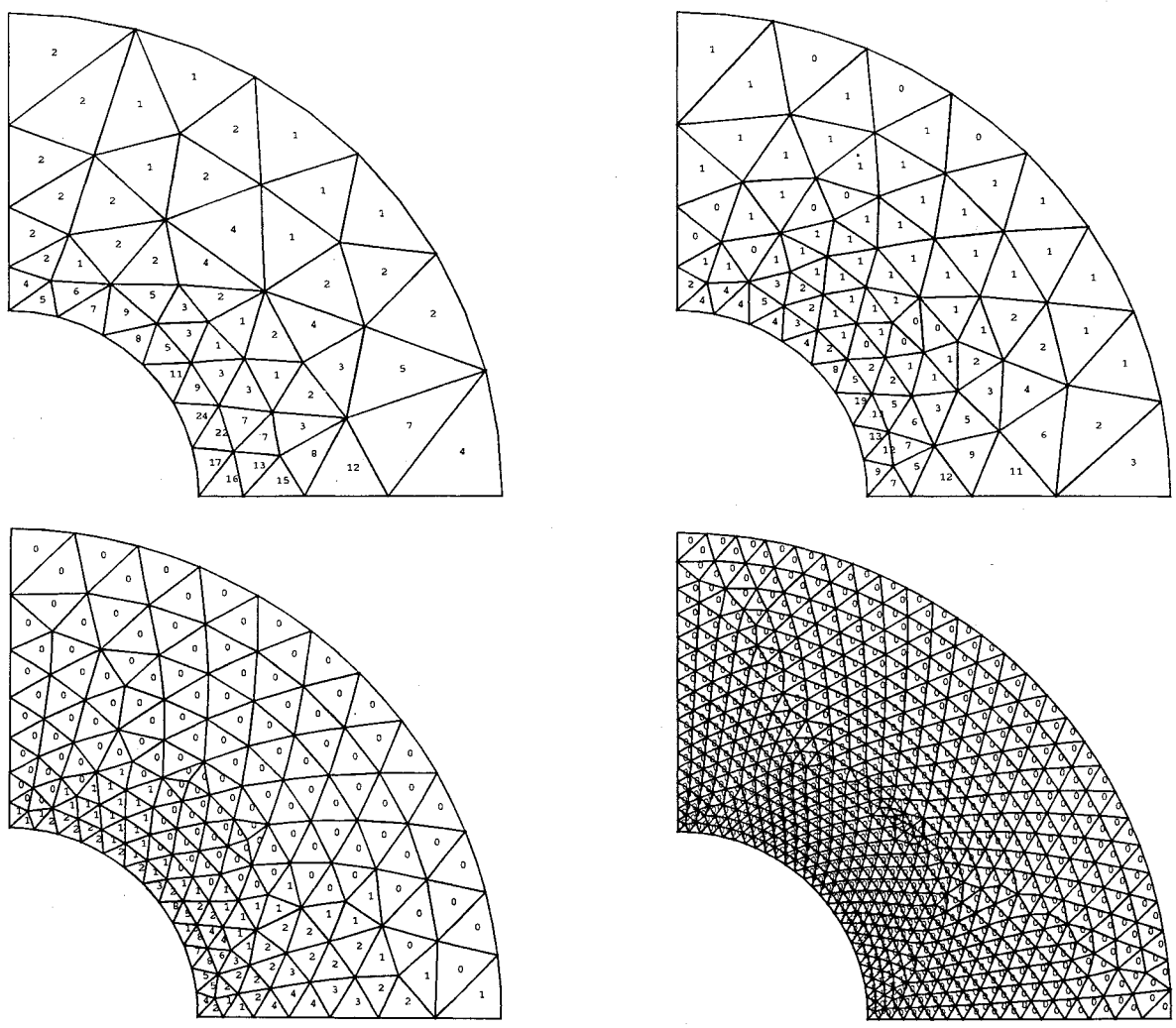

Fig. 2 Refined meshes with elemental error estimates with 1362, 2150, 5606, and 9958 DOF.

Table 7 Results for a locally refined 10:1 model with a moving internal boundary

DOF	Max. elem. error, %	$(\sigma_x)_{max}$, psi	Stress error, %
1,328	65.7	3,055	85.35
1,668	64.2	4,546	78.20
1,876	71.3	8,393	59.76
1,784	53.5	12,000	42.46
1,624	33.6	14,771	29.18
1,570	25.8	16,043	23.08
3,450	18.8	17,720	15.04
7,450	11.2	19,110	8.37
5,430	0.6	20,039	3.92

of 20,039 psi is predicted. This is 3.92% less than the analytic result. This result was achieved with a mesh of 5430 DOF and a maximum elemental error of 0.8%.

Summary, Conclusions, and Recommendations for Further Research

A submodeling approach for adaptively refining stress concentrations has been developed. The stress concentrations are separated from the remainder of the problem one at a time by defining internal boundaries in terms of elemental error measures. The fact that the effects of the remainder of the problem are satisfactorily included in the subproblem by interpolating the displacements across the internal boundary is indicated by the accuracy of the results.

The adaptive refinement is terminated when the maximum elemental error reaches a predetermined value. This contrasts to some approaches where a global error measure is used to terminate the analysis. The use of the elemental error measure to stop the analysis removes the effect of the far-field elements from the assessment of the accuracy of the results at the stress concentration. The accuracy of the analysis in the region of interest is used to terminate the analysis.

The adaptive refinement of a submodel containing a stress concentration allows the computational resources to be focused on the regions of the problem where they can best be utilized. For instance, if a problem has several high-stress regions, each one can be treated separately and in detail. The 5% elemental error criterion used here to define both the internal boundary and to terminate the analysis was chosen arbitrarily. Previous experience had shown that this value would produce well-converged results for the example problems solved here. That is to say, accuracy would prevail over efficiency. Thus, a valuable area of future research would be to determine a process for identifying the criteria that would produce the desired mix between accuracy and efficiency for general problems.

References

[1]Zienkiewicz, O. C., and Zhu, J. Z., "A Simple Error Estimator and Adaptive Procedure for Practical Engineering Analysis," *International Journal for Numerical Methods in Engineering*, Vol. 24, 1987, pp. 337–357.

[2]Dow, J. O., Harwood, S. A., Jones, M. S., and Stevenson, I., "Validation of a Finite Element Error Estimator," *AIAA Journal*, Vol. 29, No. 10, 1991, pp. 1736–1742.

[3]Zienkiewicz, O. C., and Zhu, J. Z., "Superconvergent Recovery Techniques and A-Posterori Error Estimation in the Finite Element Method, Parts I and II," *International Journal for Numerical Methods in Engineering*, Vol. 33, 1992, pp. 1331–1382.

[4]Sandor, M. J., "Sub-Model Boundary Identification for Use in a Global/Local Adaptive Refinement Technique," M.S. Thesis, Univ. of Colorado, Boulder, CO, Aug. 1993.

[5]Young, W. C., *Roark's Formulas for Stress and Strain*, Sixth ed., McGraw–Hill, New York, 1989, p. 725.

[6]Dow, J. O., and Byrd, D. E., "The Identification and Elimination of Artificial Stiffening Errors in Finite Elements," *International Journal for Numerical Methods in Engineering*, Vol. 26, March 1988, pp. 743–762.